Extraction of temperature dependences of small-signal model parameters in SiGe HBT HICUM model*

Ya-Bin Sun(孙亚宾)[1], Jun Fu(付军)[2,†], Yu-Dong Wang(王玉东)[2], Wei Zhou(周卫)[2], Wei Zhang(张伟)[2], and Zhi-Hong Liu(刘志弘)[2]

[1] *College of Electronic Science and Engineering, Nanjing University of Posts and Telecommunications, Nanjing* 210003, *China*
[2] *Tsinghua National Laboratory for Information and Technology, Institute of Microelectronics, Tsinghua University, Beijing* 100084, *China*

(Received 4 November 2015; revised manuscript received 29 December 2015; published online 25 February 2016)

In this work, temperature dependences of small-signal model parameters in the SiGe HBT HICUM model are presented. Electrical elements in the small-signal equivalent circuit are first extracted at each temperature, then the temperature dependences are determined by the series of extracted temperature coefficients, based on the established temperature formulas for corresponding model parameters. The proposed method is validated by a $1 \times 0.2 \times 16$ μm^2 SiGe HBT over a wide temperature range (from 218 K to 473 K), and good matching is obtained between the extracted and modeled results. Therefore, we believe that the proposed extraction flow of model parameter temperature dependence is reliable for characterizing the transistor performance and guiding the circuit design over a wide temperature range.

Keywords: temperature dependence, model parameter, SiGe HBT, HICUM

PACS: 85.30.De, 73.40.Lq **DOI:** 10.1088/1674-1056/25/4/048501

1. Introduction

Because of its excellent performance and compatibility with conventional Si CMOS processing, SiGe HBT technology has recently received a great deal of attention in radio frequency (RF), microwave and extreme environment applications.[1,2] Since the existence of bandgap-engineering in the base region, the narrowed-bandgap induced by the Ge profile retards the classical problems associated with cooling conventional transistors, such as base freezeout, carrier diffusivity and mobility degradation.[3–5] As a consequence, nearly all the transistor metrics improve with temperature decreasing, which enables SiGe HBT to operate well in a low temperature range. Obviously, on the other hand, SiGe HBTs also suffer some degradations in AC and DC characteristics as temperature increases.[3,6,7] However, it is lucky to find that the speed of such a degradation is not very fast. For example, even at 300 °C IBM the 2nd generation SiGe HBT also possesses a current gain of above 100 and f_T above 75 GHz.[8] It demonstrates a potential of SiGe HBT operating over a wide range of temperature. Therefore, it is vital to investigate the physics of SiGe HBT model parameters over a wide temperature, and also important to build the temperature dependences of model parameters with good fidelity.

A completed transistor model generally includes two parts: the small-signal model and the large-signal model.[9] The small-signal model is a linear approximation of the large-signal model in a given bias condition and can accurately describe the transistor characteristics. The extraction of small-signal model parameters is less complicated, and it is promising to obtain the large-signal model parameters. Therefore, the temperature dependences of model parameters related to the small-signal equivalent circuit are presented in this work. The small-signal electrical elements in the SiGe HBT HICUM model in off-state are first extracted at a given temperature, and the corresponding temperature coefficients for each model parameter are then obtained based on the proposed temperature formulas. This paper provides a theoretical guide for designing the device and circuit of SiGe HBTs working in a wide temperature range.

2. Experiment

After the bias-independent extrinsic parasitic elements are removed through a standard 'open' and 'short' de-embedding pattern, the small-signal equivalent circuit of the SiGe HBT HICUM model under cut-off mode is obtained, as shown in Fig. 1.[10] The temperature dependences of resistance and capacitance originate from the physical quantities such as the intrinsic carrier density, diffusivity or mobility. The temperature coefficients related to the model parameters in Fig. 1 are respectively the effective bandgap voltages V_{gEeff}, V_{gCeff}, and V_{gSeff}, temperature exponents $\zeta_{R_{\mathrm{B}}}$ for base resistance, $\zeta_{R_{\mathrm{CX}}}$ for collector resistance, $\zeta_{R_{\mathrm{SU}}}$ for substrate resistance, and $\zeta_{R_{\mathrm{E}}}$ for emitter resistance.

The devices under test are vertical NPN SiGe HBTs and five temperature points 218 K, 248 K, 298 K, 373 K, and 473 K are adopted. DC characteristics including the forward-

*Project supported partially by the Important National Science & Technology Specific Projects, China (Grant No. 2013ZX02503003).
†Corresponding author. E-mail: fujun@tsinghua.edu.cn
© 2016 Chinese Physical Society and IOP Publishing Ltd

Gummel and R_C_flyback are measured with an Agilent B1500 Semiconductor Parameter Analyzer, and the S-parameter measurements are carried out in a microwave probing system using a vector network analyzer over a frequency range of 100 MHz–25 GHz.

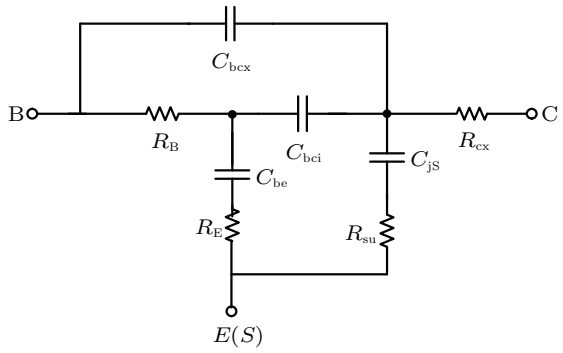


Fig. 1. Simplified small-signal equivalent circuit in SiGe HBT HICUM model biased at off-state.

3. Extraction of electrical elements

The junction capacitances are first extracted from the cold S-parameters measurement.[11] For the BE junction capacitance C_{be} and BC junction capacitance C_{bc}, base voltage V_B is swept from -1 V to 0.4 V under a fixed $V_C = 0$ V. Similarly, for the CS junction capacitance C_{jS}, V_C is swept from -0.4 V to 1.5 V with a constant $V_B = V_S = 0$ V. Then the junction capacitance can be directly determined from the following non-linear rational function fitting over the whole frequency range:[11]

$$\begin{aligned}&\mathrm{Im}(Y_{11}+Y_{12})\\ &= \frac{C_{be}\omega + N_{11}\omega^3 + N_{12}\omega^5 + N_{13}\omega^7}{1 + M_{11}\omega^2 + M_{12}\omega^4 + M_{13}\omega^6 + M_{14}\omega^8},\end{aligned} \tag{1}$$

$$\begin{aligned}&\mathrm{Im}(-Y_{12})\\ &= \frac{(C_{bci}+C_{bcx})\omega + N_{31}\omega^3 + N_{32}\omega^5 + N_{33}\omega^7}{1 + M_{11}\omega^2 + M_{12}\omega^4 + M_{13}\omega^6 + M_{14}\omega^8},\end{aligned} \tag{2}$$

$$\begin{aligned}&\mathrm{Im}(Y_{11}+Y_{22})\\ &= \frac{C_{jS}\omega + N_{51}\omega^3 + N_{52}\omega^5 + N_{53}\omega^7}{1 + M_{11}\omega^2 + M_{12}\omega^4 + M_{13}\omega^6 + M_{14}\omega^8}.\end{aligned} \tag{3}$$

The coefficients N_{ij} and M_{ij} of other high-order terms each are a function of the circuit elements in Fig. 1. Figure 2 shows the variations of $\mathrm{Im}(Y_{11}+Y_{12})$, $\mathrm{Im}(-Y_{12})$, and $\mathrm{Im}(Y_{22}+Y_{12})$ with angular frequency ω for $1\times0.2\times16$ μm^2 SiGe HBT biased at $V_B = V_C = 0$ V at room temperature. Excellent agreement is found over the whole frequency range, and the junction capacitances are respectively obtained to be 55.64 fF (55.04 fF, 56.24 fF) for C_{be}, 62.78 fF (61.95 fF, 63.21 fF) for $C_{bcx}+C_{bci}$, and 26.10 fF (25.92 fF, 26.28 fF) for C_{ts}. Confidence intervals (included in the above brackets) are narrow and hence the extracted junction capacitances are credibly accurate. For each operation point and measurement temperature, an appropriate fitting frequency range is adopted to obtain the global junction capacitance. As a consequence, the bias-dependent junction capacitances at different temperatures are determined, then the junction capacitance model parameters, zero-biased depletion capacitances, grading coefficients, and built-in voltage are obtained, which will be discussed in the following section.

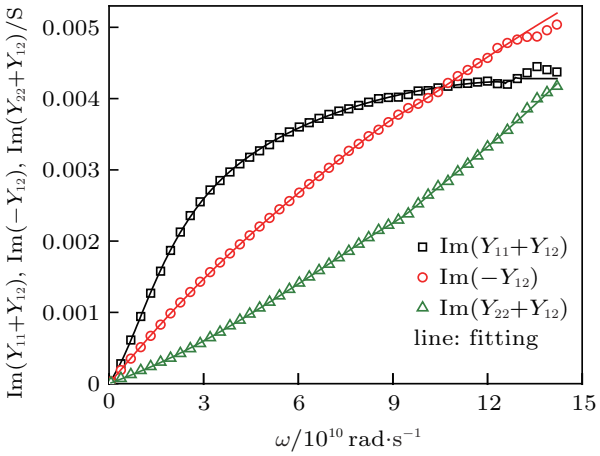


Fig. 2. (color online) Comparison between the measured (symbols) and fitting results (solid lines) of formulas (1)–(3) for $1\times0.2\times16$ μm^2 SiGe HBT biased at $V_B = V_C = 0$ V at room temperature.

The substrate resistance R_{SU} can be extracted by using the reported cold S-parameter approach.[12] The external collector resistance R_{CX} can be determined through the convenient flyback method.[13] As for the emitter resistance R_E, a novel extraction method has been proposed based on forward-Gummel measurements in our pervious study.[14] In the medium current region we can obtain

$$\frac{\partial \ln(I_B)}{\partial V_{BE}} = \frac{q}{kT} - \frac{qR_E}{kT}\frac{\partial I_E}{\partial V_{BE}}, \tag{4}$$

where V_{BE} represents the applied voltage across the BE junction, kT/q is the thermal voltage at given temperature T, I_B, and I_E are base current and emitter current in the forward Gummel measurement, R_E can be determined from the least squares linear fitting of Eq. (4) when plotting $\partial\ln(I_B)/\partial V_{BE}$ versus $\partial I_E/\partial V_{BE}$, as shown in Fig. 3, from which an almost straight line is expected in the medium current region for a $1\times0.2\times16$ μm^2 SiGe HBT at room temperature. It is demonstrated that expression (4) is reasonable and the extracted R_E values are reliable. The deviation between the measured and fitted data in the high current region is due to the high injection and quasi-saturation effects. For example, the heterojunction barrier effect (HBE) and self-heating effect will lead to a slower increasing speed of I_C (or I_E) than that of I_B with V_{BE} increasing, thus a large deviation appears in the plot of the high current region, as shown in Fig. 3. Therefore, the proposed method avoids some losses of extraction precision induced by the high current effect.

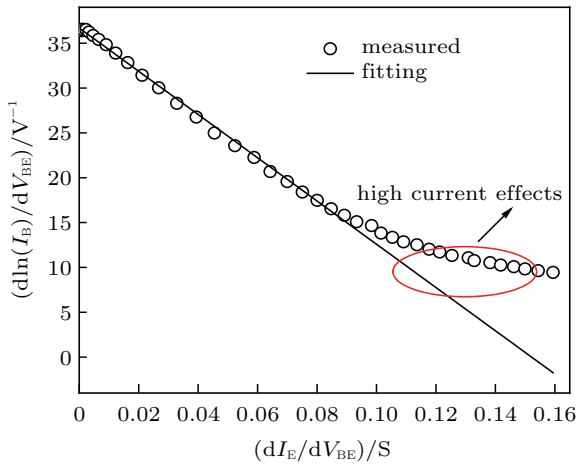


Fig. 3. (color online) Typical fitting result of Eq. (4) for a $1\times0.2\times16$ μm^2 SiGe HBT.

As in our pervious study, the remaining model parameter R_B can be obtained based on the nonlinear rational function fitting.[15] Taking a $4\times1.2\times20$ μm^2 SiGe HBT under off-states for example, as shown in Fig. 4, R_B and R_CX both decrease with the external BC junction C_bcx increasing. R_B is confined within a narrow range from 9.88 Ω to 10.59 Ω when R_CX drops to zero. Then with the aid of pre-determined R_CX of 4.18 Ω (already extracted from R_C_flyback method), R_B is obtained to be 10.17 Ω. In other words, the base resistance here is directly extracted from cold S-parameters without making any numerical optimization.

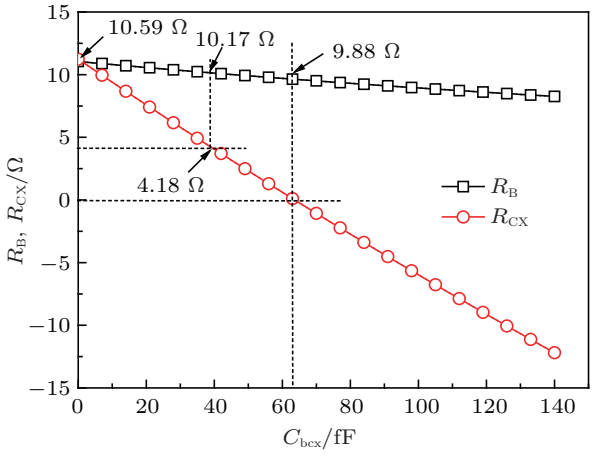


Fig. 4. (color online) Plots of R_B and R_CX versus C_bcx for $4\times1.2\times20$ μm^2 SiGe HBT in cut-off state.

Through the given method as discussed above, the series resistances R_CX, R_SU, R_E, and R_B at each temperature can be extracted and the plots will be given below. By far, the problem of extracting each electrical element in the small-signal equivalent-circuit as shown in Fig. 1 has been completed. Then based on these extracted results at each temperature, the temperature dependence can be established, which will be discussed in the following section.

4. Temperature dependence of model parameters

In the HICUM model, the temperature dependence of model parameters is described via the physical quantities such as intrinsic carrier density, diffusivity or mobility. The temperature dependence of internal base resistance R_B here depends on the carrier mobility in the neutral region. Then zero-bias resistance is described as:[16]

$$R_\mathrm{B}(T)=R_\mathrm{B}(T_0)\left(\frac{T}{T_0}\right)^{\zeta_{R_\mathrm{B}}}, \tag{5}$$

where T_0 is the reference temperature and $R_\mathrm{B}(T_0)$ is the determined base resistance at given temperature T_0. The temperature coefficient ζ_{R_B} is a function of base doping concentration. The external collector resistance R_CX, emitter resistance R_E, and substrate resistance R_SU each follow a similar relationship to that shown in Eq. (5). The temperature coefficients ζ_{R_CX}, ζ_{B_E}, and ζ_{R_SU} each are a function of average doping concentration in a corresponding region.

As in Ref. [11], all junction depletion capacitances are modeled in terms of the capacitance at zero bias C_j0, a built-in voltage V_D and a grading coefficient z_j. In HICUM the grading coefficient z_j is assumed to be a constant and temperature-independent. To access the temperature dependence of built-in voltage V_D, an auxiliary voltage $V_\mathrm{Dj}(T_0)$ at given reference temperature T_0 is calculated as indicated in Ref. [16] and given as follows:

$$V_\mathrm{Dj}(T_0)=2V_{T0}\ln\left[\exp\left(\frac{V_\mathrm{D}(T_0)}{2V_{T0}}\right)-\exp\left(-\frac{V_\mathrm{D}(T_0)}{2V_{T0}}\right)\right], \tag{6}$$

where $V_\mathrm{D}(T_0)$ and V_{T0} are the built-in voltage and thermal voltage at reference temperature T_0 respectively. With the linear temperature-dependent effective bandgap, the value $V_\mathrm{Dj}(T)$ at an arbitrary temperature is written as[16]

$$\begin{aligned}V_\mathrm{Dj}(T) &= V_\mathrm{Dj}(T_0)\frac{T}{T_0}-m_\mathrm{g}V_T\ln\left(\frac{T}{T_0}\right)\\ &\quad -V_\mathrm{geff}(0)\left(\frac{T}{T_0}-1\right),\end{aligned} \tag{7}$$

where m_g is a constant to characterize the temperature dependence of the intrinsic carrier density and $V_\mathrm{geff}(0)$ is the finite bandgap at $T=0$ K. Finally, the built-in voltage $V_\mathrm{D}(T)$ can be calculated as[16]

$$\begin{aligned}&V_\mathrm{D}(T)\\ &=V_\mathrm{Dj}(T)+2V_T\ln\left(\frac{1}{2}\left[1+\sqrt{1+4\exp\left(-\frac{V_\mathrm{Dj}(T)}{V_T}\right)}\right]\right).\end{aligned} \tag{8}$$

It is noted that the built-in voltage V_D is associated with the relevant junction region, for example, V_de is related to the base

and emitter region, therefore $V_{\rm geff}$ here should be an average effective bandgap, which is written as[16]

$$V_{\rm geff} \approx V_{\rm g(x,y)eff} = \frac{V_{\rm gxeff} + V_{\rm gyeff}}{2}, \tag{9}$$

with $(x,y) =$ (B, E), (B, C), (C, S). Generally, the depletion junction $C_{\rm j0}$ at zero bias is expressed as $C_{\rm j0} \sim V_{\rm D}^{-z}$, therefore, the temperature dependence of $C_{\rm j0}$ can be directly obtained from the previously determined $V_{\rm D}$, and expressed as

$$C_{\rm j0}(T) = C_{\rm j0}(T_0)\left(\frac{V_{\rm D}(T_0)}{V_{\rm D}(T)}\right)^{Z_{\rm j}}. \tag{10}$$

The grading coefficient z here does not depend on temperature. As reported in Ref. [11], the well-known junction depletion capacitances can be modeled, respectively, as

$$C_{\rm be} = \frac{C_{\rm be0}}{(1 - V_{\rm BE}/V_{\rm dE})^{z_{\rm de}}}, \tag{11}$$

$$C_{\rm bc} = \frac{C_{\rm bci0}}{(1 - V_{\rm BC}/V_{\rm dC})^{z_{\rm dc}}} + C_{\rm bcx}, \tag{12}$$

$$C_{\rm jS} = \frac{C_{\rm jS0}}{(1 - V_{\rm SC}/V_{\rm dS})^{z_{\rm ds}}}, \tag{13}$$

where $C_{\rm be0}$, $C_{\rm bci0}$, $C_{\rm jS0}$ are the zero-biased depletion capacitances; $Z_{\rm de}$, $Z_{\rm dc}$, $Z_{\rm dS}$ are the grading coefficients; $V_{\rm dE}$, $V_{\rm dC}$, and $V_{\rm dS}$ are the built-in voltages of BE junction, BC junction, and CS junction, respectively; and $V_{\rm BE}$, $V_{\rm BC}$, and $V_{\rm SC}$ are the applied forward bias voltage across the junctions. Here the external BC junction $C_{\rm bcx}$ is assumed to be bias-independent.

It is noted that the built-in voltage $V_{\rm D}$ is temperature dependent and the grading coefficient $Z_{\rm d}$ is temperature-independent in the HICUM model, therefore, $V_{\rm D}$ cannot be set as a constant similar to the case at room temperature. A novel parameter extraction flow for the depletion capacitances is recommend. First, the C–V characteristics at given reference temperature T_0 is fitted directly, then the built-in voltage $V_{\rm D}$, zero-biased capacitance $C_{\rm j0}$ and grading coefficient $Z_{\rm d}$ will be obtained simultaneously if high accuracy exists. Otherwise, set $V_{\rm D}$ as the default value, and extract the $C_{\rm j0}$ and $Z_{\rm d}$ from the C–V curve fitting. Finally, the values of $V_{\rm D}$ and $C_{\rm j0}$ at different temperatures can be determined from the corresponding C–V curve fitting under the assumption of $Z_{\rm d}(T) = Z_{\rm d}(T_0)$. Thus, the temperature dependences of $V_{\rm D}(T)$ and $C_{\rm j0}(T)$ are obtained.

In HICUM the temperature dependence of model parameters is assumed to be irrelevant to device size, therefore, the extraction of temperature dependence for a single transistor geometry can also be applied to other-sized devices. The results for a $1 \times 0.2 \times 16$ μm^2 SiGe HBT are presented in this work. According to Eqs. (6)–(13), the obtained relative temperature coefficients are shown in Table 1. The variations of built-in voltage $V_{\rm D}$ and zero-biased depletion capacitances $C_{\rm j0}$ for BE junction, BC junction, and CS junction, with temperature are shown in Figs. 5–7, respectively. Excellent agreement is obtained between the extracted and fitted model parameters at most temperature points.

The temperature dependences of series resistances ($R_{\rm B}$, $R_{\rm CX}$, $R_{\rm E}$, and $R_{\rm SU}$) are shown in Fig. 8, from which good agreement is obtained over the whole measurement temperature range from 218 K to 473 K. Besides, it is found that the variation tendency of $R_{\rm E}$ is different from those of the other three resistances as temperature increases. $R_{\rm B}$, $R_{\rm CX}$, and $R_{\rm SU}$ gradually increase while $R_{\rm E}$ decreases with temperature increasing, which may be due to the different scattering mechanisms contributing to carrier mobility.[9]

Table 1. Extracted temperature coefficients for $1 \times 0.2 \times 16$ μm^2 SiGe HBT.

$Z_{\rm dei}$	$V_{\rm gEeff}$/V	$Z_{\rm dci}$	$V_{\rm gCeff}$/V	$Z_{\rm dsi}$	$V_{\rm gSeff}$/V
0.184	0.949	0.2715	0.9174	0.06075	0.8136
$m_{\rm g}$	$\zeta_{R_{\rm B}}$	$\zeta_{R_{\rm E}}$	$\zeta_{R_{\rm CX}}$	$\zeta_{R_{\rm SU}}$	
3	0.6283	−0.3456	0.7533	0.6049	

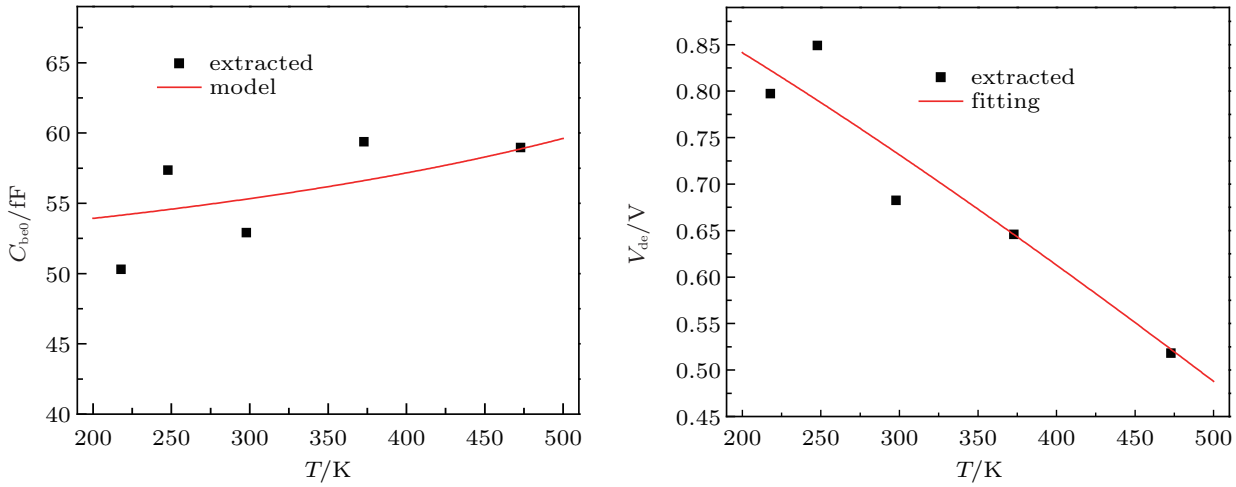


Fig. 5. (color online) Temperature dependences of zero-bias capacitance and built-in voltage for BE junction.

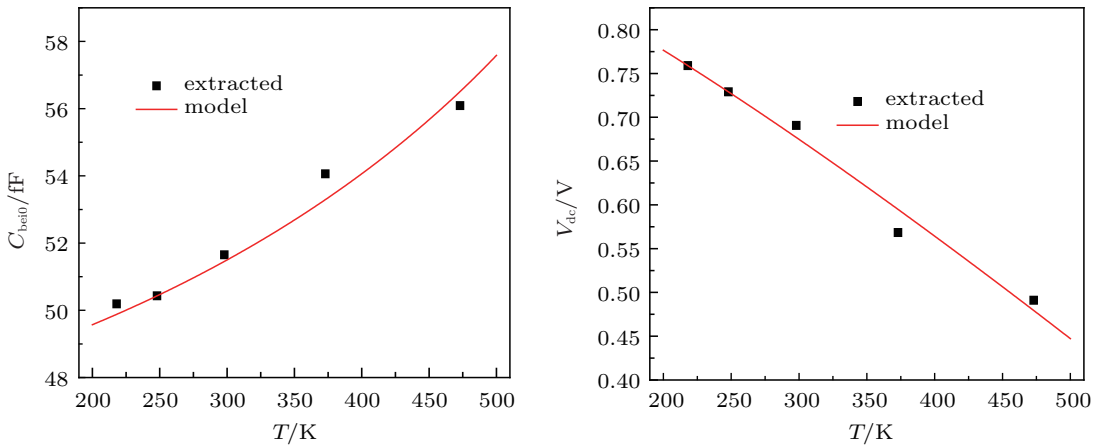


Fig. 6. (color online) Temperature dependences of zero-bias capacitance and built-in voltage for BC junction.

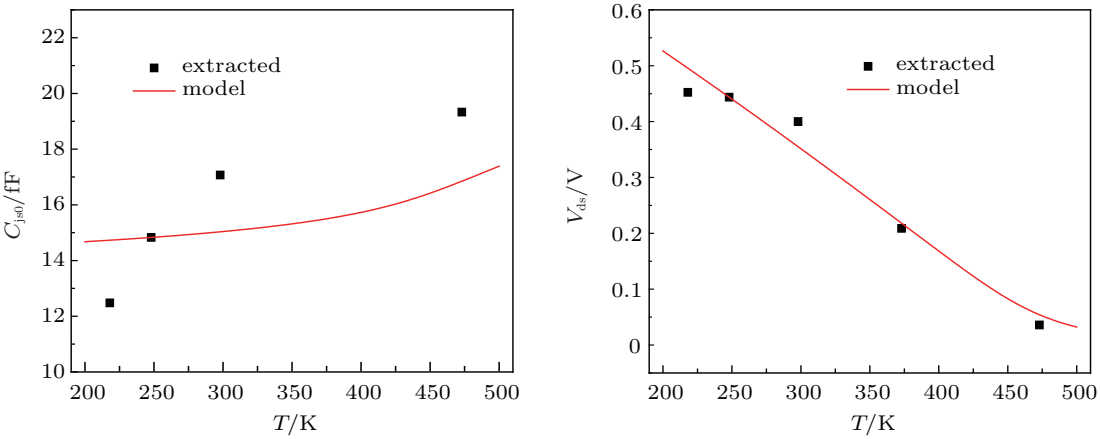


Fig. 7. (color online) Temperature dependences of zero-bias capacitance and built-in voltage for CS junction.

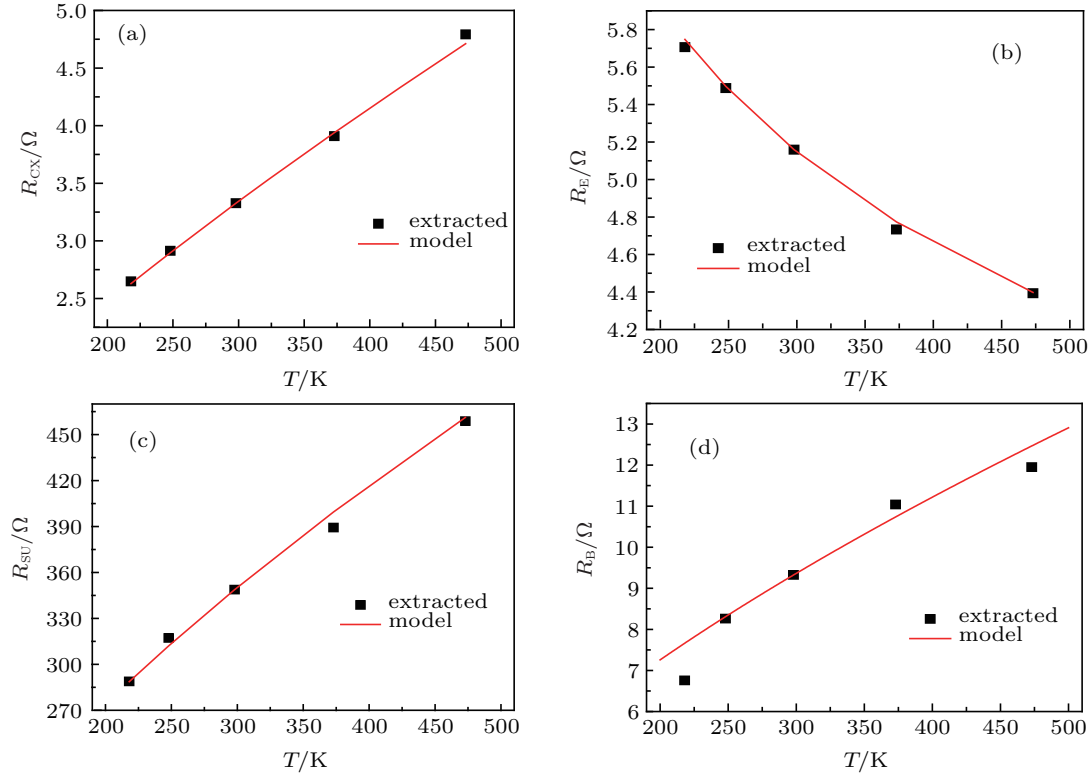


Fig. 8. (color online) Temperature dependences of series resistances of (a) R_{CX}, (b) R_E, (c) R_{SU}, and (d) R_B.

Because of the low doping concentration, the carrier mobilities in base, collector and substrate region are mainly dominated by the lattice vibration scattering, which shows a temperature dependence of $T^{3/2}$ and increases with temperature increasing. Therefore, the carrier mobility in these regions decreases and the corresponding series resistances increase as temperature increases. While in the emitter region, it is the ionized impurity scattering that dominates the carrier mobility due to the higher doping concentration (generally at a level of 10^{20} cm^{-3}). The ionized impurity scattering shows a temperature dependence of $T^{3/2}$ and hence decreases with temperature increasing; as a result, the carrier mobility in the emitter region increases and then the emitter resistance R_{E} decreases.

5. Conclusions

In this paper, the temperature dependences of small-signal model parameters for SiGe HBT HICUM under cut-off mode are presented from 218 K to 473 K. The depletion capacitances are extracted from the cold *S*-parameter measurements. Emitter resistance R_{E} is obtained from the forward-Gummel measurement. Base resistance R_{B} is gained from cold *S*-parameters based on the rational function fitting. Then the temperature dependences of model parameters are determined based on the established temperature formulas. The proposed method is verified with a $1 \times 0.2 \times 16$ μm^2 SiGe HBT and good agreement is obtained over the whole temperature range. These results provide a theoretical guide for designing devices and circuits of SiGe HBTs in a wide temperature range.

Acknowledgment

The authors would like to thank the Shanghai Huahong Grace Semiconductor Manufacturing Corporation for fabricating SiGe HBTs under test..

References

[1] Sun Y B, Fu J, Xu J, Wang Y D, Zhou W and Zhang W 2014 *Chin. Phys. B* **23** 116104

[2] Sun Y B, Fu J, Xu J, Wang Y D, Zhou W and Zhang W 2013 *Acta Phys. Sin.* **62** 196104 (in Chinese)

[3] Cressler J D 2010 *IEEE Trans. Dev. Mater. Rel.* **10** 437

[4] Cui Y, Niu G F, Shi Y, Zhu C D, Najafizadeh L, Cressler J D and Joseph A 2006 *IEEE Bipolar/BiCMOS Circuits Technol. Meeting*, p. 1

[5] Bhaskar B, Venkataraman S, Yuan L, Liang Q, Lee C, Nuttinck S, Dekhyuon H, Chen Y, Cressler J D, Laskar J, Freeman G and Ahlgren D C 2005 *IEEE Trans. Electron Dev.* **4** 585

[6] Chen T, Kuo W L, Zhao E, Liang Q, Jin Z, Cressler J D and Joseph A J 2004 *IEEE Trans. Electron Dev.* **11** 1825

[7] Thomas D B, Najafizadeh L, Cressler J D, Moen K A and Lourenco N 2011 *Solid-State Electron.* **56** 47

[8] Yuan J, Cressler J D, Krithivasan R, Thrivikraman T, Khater M H, Ahlgren D C, Joseph A J and Rieh J 2009 *IEEE Trans. Electron Dev.* **56** 1007

[9] Cressler J D and Niu G F 2003 *Silicon-germanium heterojunction bipolar transistors* (Norwood: Artech House)

[10] Schrer M and Chakravorty A 2010 *Compact hierarchical modeling of bipolar transistors with HICUM* (Singapore: World Scientific)

[11] Raya C, Schwartzmann T, Chevalier P, Pourchon F, Celi D and Zimmer T 2007 *IEEE Bipolar/BiCMOS Circuits Technol. Meeting*, p. 188

[12] Basaran U and Berroth M 2003 *IEEE Bipolar/BiCMOS Circuits Technol. Meeting*, p. 93

[13] Gabl R and Reisch M 1998 *IEEE Trans. Electron Dev.* **12** 2457

[14] Yang J, Fu J, Sun Y B, Wang Y D, Zhou W and Zhang W 2014 *IEEE International Conference on Electron Devices and Solid-State Circuits*, Chengdu, China, p. 1

[15] Sun Y B, Fu J, Yang J, Wang Y D, Zhou W and Zhang W 2014 12*th IEEE International Conference on Solid-State and Integrated Circuit Technology*, Guilin, China, p. 1

[16] Schroter M and Mukherjee A 2008 *HICUM-A Geometry Scalable Physics-Based Compact Bipolar Transistor Model*, Documentation of model level 2 version 2.23, University of Technology Dresden, Germany